Journal of Molecular Catalysis A: Chemical 302 (2009) 54–58

Contents lists available at ScienceDirect

Journal of Molecular Catalysis A: Chemical

journal homepage: www.elsevier.com/locate/molcata

Structure-dependent photocatalytic activities of MWO_4 (M = Ca, Sr, Ba)

Zhichao Shan[a,b], Yaoming Wang[a], Hanming Ding[b,*], Fuqiang Huang[a,*]

[a] State Key Laboratory of High Performance Ceramics and Superfine Microstructures, Shanghai Institute of Ceramics, Chinese Academy of Sciences, Shanghai 200050, PR China
[b] Department of Chemistry, East China Normal University, Shanghai 200062, PR China

ARTICLE INFO

Article history:
Received 9 July 2008
Received in revised form
25 November 2008
Accepted 26 November 2008
Available online 3 December 2008

Keywords:
Photocatalysis
Packing factor
MWO_4 (M = Ca, Sr, Ba)
Methyl orange

ABSTRACT

The photocatalytic activities of the isostructural photocatalysts MWO_4 (M = Ca, Sr, Ba) for decomposing methyl orange, which were synthesized by a solid state reaction, were investigated. In the experiments, the photocatalytic activity is in the increasing order of $CaWO_4 < SrWO_4 < BaWO_4$ under both neutral and acidic conditions. The factors, which influence the photocatalytic processes and the final activity, were analyzed the difference of their photocatalytic behaviors. The further investigation indicates that the higher structural openness degree, corresponding to a lower packing factor, leads to the better photocatalytic activity.

1. Introduction

Photocatalytic decomposition of pollutants in air and water belongs to one of the most promising methods for environment-organic-pollutant decontamination. In the past three decades, the semiconductor photocatalysts have attracted much attention, because their advantages such as unlimited resources, low cost, and environmental friendliness. Therefore, in order to search an effective photocatalyst a tremendous amount of research has been devoted to study and discover the influencing factors of the photocatalytic activity.

Irradiation of a semiconductor with light of energy equal to or larger than the band gap energy leads to the generation of electron–hole pairs, which can subsequently induce redox reactions on the semiconductor surface. An ideal photocatalyst should possess a high mobility for photostimulated electron–hole separation and transportation in crystal lattices and suitable energy levels of band potentials. This is one of the most significant considerations as a semiconductor is chosen for the photocatalytic application.

It is thought that the photocatalytic performance or the electron–hole separation ability of a semiconductor is closely related to the crystal structure. So, many studies [1–10] have been reported on the relationship between crystal structure and the photocatalytic properties. The proposed principles are that the local electric fields or polarized fields in the distorted metal-oxygen polyhedra are positive for the efficient photoexcitation, delocalization and migration of charges [1–10]. For example, the presence of the dipole moments in heavily distorted $[MO_6]$ (M = In, Ga, Fe, Ta) octahedra in the photocatalysts Bi_2MTaO_7 (M = In, Ga, Fe) [4]. Besides that, the polarized fields are also found in heavily distorted $[TiO_6]$ octahedra in the typical tunneled structure compounds, $A_2Ti_6O_{13}$ (A = Na, K, Rb) and $BaTi_4O_9$, to contribute to high catalytic performances [5–7].

The interior electric fields in some layered structure materials also favor charge separation, and contribute to enhance the photocatalytic activity. For example, in the Bi_3O_4Cl semiconductor, the $[Bi_3O_4]$ and [Cl] slices are one-by-one orderly stacked to form the unique layered structure. The permanent static electric fields between $[Bi_3O_4]$ and [Cl] layers can work as accelerators for the separations of electron–hole pairs upon photoexcitation to favor a high photocatalytic efficiency of Bi_3O_4Cl [8]. Thus, layered structure compounds are also expected to be important materials for photocatalysis. On the basic of this model a series compounds with layered structure, e.g. $Bi_2W_2O_9$ [9] and BiOCl [10], have been studied as high-performance photocatalysts. Moreover, as we all know that many other important effects, such as particle size, band gap, band structure, phase purity, surface area, and morphology, etc., have been also systematically studied.

Besides, in our previous work [11,12], crystal packing factor (PF) as a criterion was introduced to analyze the photocatalytic difference of materials with similar band structure (similar crystal structure or chemistry). The PF effects of photocatalysts on MO decomposition could be discussed based on the lifetime and mobility

* Corresponding authors. Tel.: +86 21 52411620; fax: +86 21 52413903.
E-mail addresses: hmding@chem.ecnu.edu.cn (H. Ding), huangfq@mail.sic.ac.cn (F. Huang).

1381-1169/$ – see front matter © 2008 Elsevier B.V. All rights reserved.
doi:10.1016/j.molcata.2008.11.030

of electrons and holes. It is conceivable that a structure with a lower PF is more polarizable, therefore its exciton radius is larger and the lifetimes of electrons and holes are longer. Meanwhile, a structure with lower PF is more deformable, which lowers the activation barrier for polarons and thus their mobility are increased.

In crystallography, packing factor is the fraction of volume in a crystal structure that is occupied by atoms. For practical purposes, the PF of a crystal structure is determined by assuming that atoms are rigid spheres. It is represented mathematically by

$$\mathrm{PF} = \frac{Z(aV_A + bV_B + cV_C)}{V_{cell}}, \quad (1)$$

where Z is the number of formula units in the unit cell; V_A, V_B, V_C are ion volumes ($V_A = 4\pi {r_A}^3/3$) (r_A is the A coordination-dependent ionic radium), and so are V_B and V_C; V_{cell} is the cell volume.

Herein, we took the isostructural MWO_4 (M = Ca, Sr, Ba) photocatalyst system as an example to investigate these factors, which influence the photocatalytic properties of the semiconductors.

2. Experimental

In general, many exterior factors influence the photocatalytic properties of various semiconductors, such as phase purity, surface area, morphology, etc., which are sufficiently taken into account and controlled by all possible means during the sample preparation. MCO_3 (Sinoreg., 99.5%) and WO_3 (Sinoreg., 99.5%) were used as raw materials to synthesize MWO_4. Mixed powders with the stoichiometric proportion were calcined at the different temperature for 10 h in an alumina crucible in air. The respective calcination temperatures were 950 °C for $CaWO_4$, $SrWO_4$, and $BaWO_4$. After grinding, the powders were retreated at same process. The formations of the metal oxides were confirmed by X-ray diffraction (Bruker D8 Advance diffractometer using Cu K_α radiation (λ = 0.15406 nm)) analysis. Optical band gaps of these three samples were estimated by UV–vis (HITACHI U-3010 spectrophotometer) diffuse reflectance spectra. Particle size and morphology were observed on a scanning electron microscope (Philip XL30 20 kV).

The UV light photocatalytic reactor consists of two parts, a quartz cell with a circulating water jacket and a 500-W high-pressure mercury lamp with a maximum emission at 365 nm placed inside the quartz cell. The volume of the initial 10 mg/L MO solution is 300 mL. The powder concentration in the MO aqueous solution is 0.20 g/100 mL. Diluted H_2SO_4 was used to adjust the pH value of the suspending solution. The UV illumination was conducted after the suspension was magnetically stirred in the dark for 60 min to reach the adsorption–desorption equilibrium of MO on catalysts. Under irradiation, about 3 mL suspension was continually taken from the reaction cell at given time intervals for subsequent MO concentration analysis after centrifuging by measuring its maximum absorption (464 nm) with a UV–vis spectrophotometer (HITACHI U-3010 spectrophotometer).

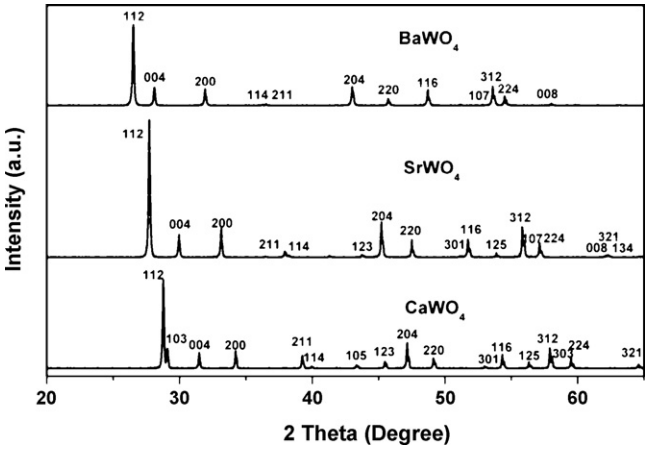

Fig. 1. XRD patterns of $CaWO_4$, $SrWO_4$ and $BaWO_4$.

3. Results and discussion

3.1. Samples characterization

As shown in Fig. 1, the $CaWO_4$, $SrWO_4$ and $BaWO_4$ samples exhibited the XRD pattern of the tetragonal crystal structure as indexed in JCPDS-ICDD 41-1431, 08-0490 and 43-0646, respectively. The XRD patterns of the samples revealed sharp and symmetric peaks, indicating the high crystallinity of the powders. With increasing ionic radii of M (from Ca to Ba), the XRD peaks shifted towards smaller angles. Correspondingly, the lattice parameters of the oxides increased in the same order from $CaWO_4$ to $SrWO_4$ and $BaWO_4$. Notice that compared to the standard data, the shift of d space toward smaller values was very small, i.e. less than 0.01 Å (see Table 1).

The particle sizes and crystallite morphologies of the $CaWO_4$, $SrWO_4$ and $BaWO_4$ compounds were examined by using scanning electron micrograph (SEM), as shown in Fig. 2. The average particle sizes are in the order of $BaWO_4$ > $SrWO_4$ > $CaWO_4$. Correspondingly, as shown in Table 2 the BET surface areas are in the order of $CaWO_4$ (0.33 m^2/g) > $SrWO_4$ (0.20 m^2/g) > $BaWO_4$ (0.13 m^2/g).

Fig. 3 shows the UV–vis diffuse reflectance spectra of the MWO_4 powder samples. The main absorption edges are 310 nm for $CaWO_4$, 318 nm for $SrWO_4$, and 313 nm for $BaWO_4$, respectively. The energy band gap was determined to be 4.00 eV for $CaWO_4$, 3.89 eV for $SrWO_4$ and 3.96 eV for $BaWO_4$, respectively.

3.2. Photocatalytic activity

Fig. 4 shows the MO photodecomposition behaviors over the catalysts as a function of UV irradiation time. Under neutral condition,

Table 1
Crystal structural parameters.

Compounds	Structure	Structural parameters (standard date)			Structural parameters (experiment date)		
		a, *b*, *c* (Å)	α, β, γ (°)	Cell volume (Å^3)	*a*, *b*, *c* (Å)	α, β, γ (°)	Cell volume (Å^3)
$CaWO_4$	Tetragonal	*a* = 5.243 *b* = 5.243 *c* = 11.374	α = 90.0 β = 90.0 γ = 90.0	312.64	*a* = 5.236 *b* = 5.236 *c* = 11.358	α = 90.0 β = 90.0 γ = 90.0	311.39
$SrWO_4$	Tetragonal	*a* = 5.417 *b* = 5.417 *c* = 11.951	α = 90.0 β = 90.0 γ = 90.0	350.66	*a* = 5.402 *b* = 5.402 *c* = 11.920	α = 90.0 β = 90.0 γ = 90.0	347.84
$BaWO_4$	Tetragonal	*a* = 5.613 *b* = 5.613 *c* = 12.720	α = 90.0 β = 90.0 γ = 90.0	400.81	*a* = 5.603 *b* = 5.603 *c* = 12.684	α = 90.0 β = 90.0 γ=90.0	398.20

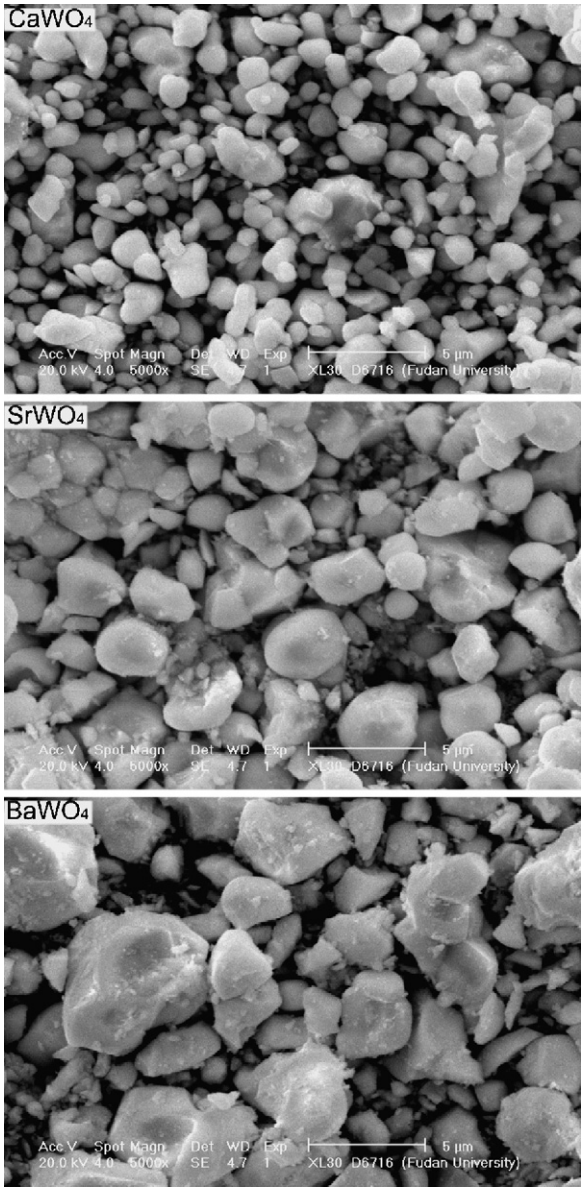

Fig. 2. Scanning electron microscopy images of $CaWO_4$, $SrWO_4$ and $BaWO_4$.

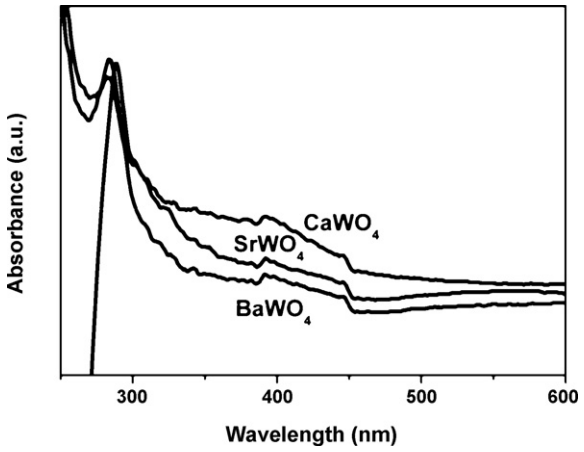

Fig. 3. UV–vis diffuse reflectance spectra of $CaWO_4$, $SrWO_4$ and $BaWO_4$.

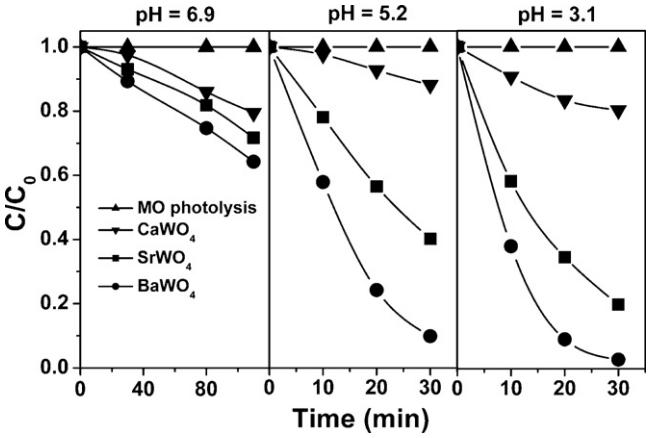

Fig. 4. MO photodegradation under UV light irradiation.

the MO photodecomposition over $BaWO_4$ after 110 min of UV light illumination is 36%, which is higher than 29% over $SrWO_4$ and 21% over $CaWO_4$.

We further examined the pH-dependent photocatalytic activities of MWO_4. The pH value shows the strong influence on the MO photodegradation efficacy. The photodegradation efficacy rises with the decreasing pH value. As shown in Fig. 4, the MO photodecolorization efficiency is greatly improved as the pH value decreases from 6.9 to 3.1. These results show that the activity of the catalysts are in the order of $BaWO_4 > SrWO_4 > CaWO_4$ both under neutral and acidic conditions.

The pH-dependent photodecomposition can be mainly attributed to the variations of surface charge properties of the photocatalyst. Consequently, this changes the absorption behavior of a dye on the catalyst surface. Since MO has an anionic configuration, its adsorption is favored in the acidic solution. It increases the oxidative degradation rate of MO, in close contact with the catalyst facilitates, by positive holes or hydroxyl radicals

Table 2
Packing factors (PF), optical band gaps and BET of as-synthesized MWO_4 (M = Ca, Sr, Ba).

Compounds	Structure	Structural parameters			PF (%)	E_g (eV)	BET (m^2/g)
		a, b, c (Å)	α, β, γ (°)	Cell volume (Å^3)			
$CaWO_4$	Tetragonal	$a = 5.236$ $b = 5.236$ $c = 11.358$	$\alpha = 90.0$ $\beta = 90.0$ $\gamma = 90.0$	311.39	67.75	4.00	0.33
$SrWO_4$	Tetragonal	$a = 5.402$ $b = 5.402$ $c = 11.920$	$\alpha = 90.0$ $\beta = 90.0$ $\gamma = 90.0$	347.84	63.51	3.89	0.20
$BaWO_4$	Tetragonal	$a = 5.603$ $b = 5.603$ $c = 12.684$	$\alpha = 90.0$ $\beta = 90.0$ $\gamma = 90.0$	398.20	57.50	3.96	0.13

upon photoexcitation. On the other hand, MO becomes unstable in acidic conditions, the λ_{max} of MO, which is commonly measured by the energy required for decomposing dye molecular structure, increases from 464 to 506 nm with the pH value decreasing from 6.9 to 3.1. This also makes the decolorization easier.

3.3. The influencing factors

There are many factors which influence the photocatalytic property of a semiconductor, such as phase purity, crystallinity, surface area, morphology, band gap, band structure, crystal structure and so forth. During the sample preparation in the present experiments, the experiment related factors were sufficiently taken into account. The pure phase MWO_4 (M = Ca, Sr, Ba) powders synthesized by a solid state reaction are well crystallized (see Fig. 1). Therefore, the phase purity and crystallinity cannot explain the photocatalytic activity difference. Surface area is widely accepted to be one of the key factors to determine the activity of a photocatalyst, because the parameter to some extent combinatively covers the effects of such exterior factors as particle size, pore volume, particle morphology, etc. Normally, a larger surface area improves the photocatalytic activity. In the present three compounds, the BET surface areas are in the decreasing order of $CaWO_4 > SrWO_4 > BaWO_4$ (see Table 2). From the viewpoint of surface area, the photocatalytic activities should have the same order. However, the result of experiment ($CaWO_4 < SrWO_4 < BaWO_4$) is the opposite. Apparently, the surface area could not account for their photocatalytic activity difference. Also, there seems to be no correlation between optical band gap (light absorption) and photocatalytic activity (see Table 2).

In the three compounds, M^{2+} ions are photocatalytically inactive while W^{6+} is photocatalytically active. The conduction band mainly consists of W 5d orbitals and the valence band is primarily composed of O 2p orbitals. Thus, the similar band structure it is considered to result in the similar electric properties and the similar interactions between the W^{6+} based catalysts and the aqueous dye (MO) solutions. This is believed to be the main reason why efforts were made to compare various photocatalysts with the same active center and the similar band structure were chosen as examples to be compared by some structure-dependent models [1–3,5–7].

The experiment-related or exterior factors mentioned above could not account for the photocatalytic activity difference of MWO_4 (M = Ca, Sr, Ba). The photocatalytic activity discrepancy can only be ascribed to the mobility difference of electron–hole separation in the three materials. It is believed that the mobility for the electron–hole separation and transportation of a semiconductor is intrinsically initiated by the detailed crystal structural properties, as suggested in literatures [1–11]. Generally, our proposed model could be suitable to explain detailed properties. The same phase of the tetragonal structure is available for $CaWO_4$, $SrWO_4$ and $BaWO_4$, with space group $I4_1/a$, as shown in Fig. 5. Each W atom is coordinated to four O anions to form a $[WO_4]$ tetrahedron with the W–O bond length of 1.78 Å in $CaWO_4$. The W atom also has some bonding contacts with another four O anions in four neighboring tetrahedra WO_4, and the W···O bonds are about 3.0 Å in $CaWO_4$. Such contacts are useful for charges to transfer or exchange via the tetrahedral $[W–O]_\infty$ network. The crystal structure suggests that the packing factor of $BaWO_4$ is 57.50%, lower than 63.51% of $SrWO_4$ and 67.75% of $CaWO_4$. Therefore the structure-openness degree is in the order of $BaWO_4 > SrWO_4 > CaWO_4$ (see Table 2). As the structure-openness degree increases, the vibratility or movability of atoms intensify, and the charge exchange or transfer via $[W–O]_\infty$ network become more spatially available. In other words, $BaWO_4$ shows the best photocatalytic performance of the three compounds owing to its highest structure-openness degree.

The structure–property relationship model works well to reveal a photocatalytic activity difference of the photocatalysts

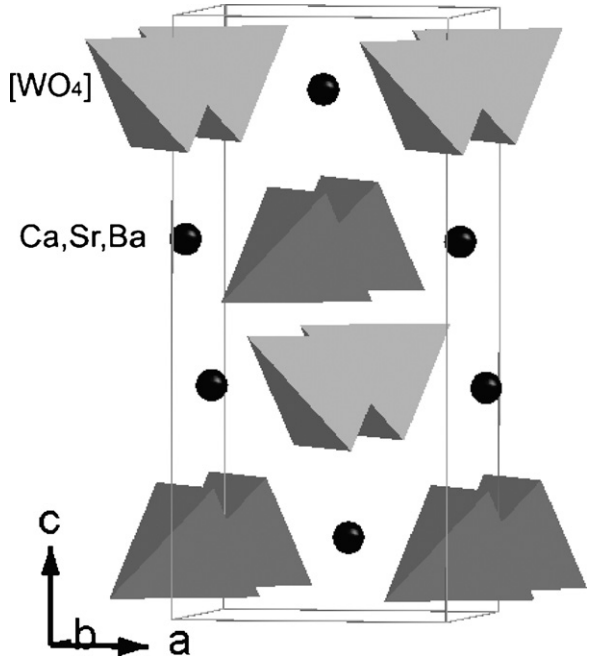

Fig. 5. Tetragonal structure of MWO_4 (M = Ca, Sr, Ba).

with similar band structure (similar crystal structure or chemistry). Besides the present result of MWO_4 (M = Ca, Sr, Ba) photocatalyst system, other examples are $SrSb_2O_7$ (64.45%) > $CaSb_2O_7$ (65.41%), $NaTi_6O_{13}$ (61.65%) > KTi_6O_{13} (63.84%) > $RbTi_6O_{13}$ (65.36%), $LiTaO_3$ (68.99%) > $NaTaO_3$ (80.46%) > $KTaO_3$ (85.03%), $BaTa_2O_6$ (62.42%) > $MgTa_2O_6$ (65.35%), $Pt/BaCrO_4$ (59.19%) > $Pt/SrCrO_4$ (61.18%), $SrIn_{0.5}Nb_{0.5}O_3$ (72.77%) > $CaIn_{0.5}Nb_{0.5}O_3$ (73.76%) > $BaIn_{0.5}Nb_{0.5}O_3$ (75.18%), and so forth [11–25].

To sum up, this macro-structural parameter (PF) in the model scales the structural openness of the semiconductor, and reflects the capacity of the metal-oxygen polyhedral deformations, the spatial amplitude of atomic vibrations in the crystal lattice, and the consequent electron–hole separation and carrier transport.

4. Conclusion

MWO_4 (M = Ca, Sr, Ba) were synthesized by a solid state reaction method. The investigation results show that their catalytic properties are in the order of $BaWO_4 > SrWO_4 > CaWO_4$ under both neutral and acidic conditions. The difference of their catalytic properties is in close connection with their micro-structural properties. The structure-openness model works well to account for such a difference. The model for structure–property relationship may be a new method to estimate the properties of photocatalysts.

Acknowledgements

The research was financially supported by National 973 Program of China Grant 2007CB936704, National Science Foundation of China Grant 50772123, Science and Technology Commission of Shanghai Grant 0752nm016 and Science and Technology Commission of Shanghai Grant 08JC1420200.

References

[1] Y. Inoue, M. Kohno, S. Ogura, K. Sato, Chem. Phys. Lett. 267 (1997) 72–76.
[2] Y. Inoue, M. Kohno, S. Ogura, K. Sato, J. Chem. Soc., Faraday Trans. 93 (1997) 2433–2437.
[3] A. Kudo, H. Kato, S. Nakagawa, J. Phys. Chem. B 104 (2000) 571–575.
[4] J. Wang, Z. Zou, J.H. Ye, J. Phys. Chem. Solids 66 (2005) 349–355.

[5] W. Hofmeister, E. Tillmanns, W.H. Bauer, Acta Crystallogr. C 40 (1984) 1510–1512.
[6] D.H. Templeton, C.H. Dauben, J. Chem. Phys. 32 (1960) 1515–1518.
[7] M. Kohno, S. Ogura, K. Sato, Y. Inoue, Chem. Phys. Lett. 319 (2000) 451–456.
[8] X.P. Lin, T. Huang, F. Huang, W.D. Wang, J. Shi, J. Phys. Chem. B 110 (2006) 24629–24634.
[9] J. Tang, J.H. Ye, J. Mater. Chem. 15 (2005) 4246–4250.
[10] K.L. Zhang, C.M. Liu, F.Q. Huang, C. Zheng, W.D. Wang, Appl. Catal. B 68 (3–4) (2006) 125–129.
[11] X.P. Lin, F. Huang, W.D. Wang, Y. Wang, Y. Xia, J. Shi, Appl. Catal. A 313 (2006) 218–223.
[12] X.P. Lin, F.Q. Huang, W.D. Wang, Z.C. Shan, J.L. Shi, Dyes Pigments 78 (2008) 39–47.
[13] J. Yin, Z. Zou, J.H. Ye, Chem. Phys. Lett. 378 (2003) 24–28.
[14] J. Sato, N. Saito, H. Nishiyama, Y. Inoue, J. Phys. Chem. B 105 (2001) 6061–6063.
[15] A. Kudo, Int. J. Hydrogen Energy 31 (2006) 197–202.
[16] T. Ishihara, N.S. Baik, N. Ono, H. Nishiguchi, Y. Takita, J. Photochem. Photobiol. A 167 (2004) 149–157.
[17] H. Kato, A. Kudo, Chem. Phys. Lett. 295 (1998) 487–492.
[18] J. Yin, Z.G. Zou, J.H. Ye, J. Phys. Chem. B107 (2003) 61–65.
[19] J.W. Liu, G. Chen, Z.H. Li, Z.G. Zhang, Int. J. Hydrogen Energy 32 (2007) 2269–2272.
[20] D. Yamasita, T. Takata, M. Hara, J.N. Kondo, K. Domen, Solid State Ionics 172 (2004) 591–595.
[21] H.Y. Song, H.F. Jiang, T. Liu, X.Q. Liu, G.Y. Meng, Mater. Res. Bull. 42 (2007) 334–344.
[22] Y. Inoue, T. Kubokawa, K. Sato, J. Phys. Chem. 95 (1991) 4059–4063.
[23] J. Tang, Z.G. Zou, J.H. Ye, Chem. Mater. 16 (2004) 1644–1649.
[24] J. Sato, H. Kobayashi, N. Saito, H. Nishiyama, Y. Inoue, J. Photochem. Photobiol. A 158 (2003) 139–144.
[25] J. Sato, N. Saito, H. Nishiyama, Y. Inoue, J. Photochem. Photobiol. A 148 (2002) 85–89.